Fabrication of tunnel barriers and single electron transistors in suspended multi-wall carbon nanotubes

Cite as: AIP Advances **9**, 105015 (2019); https://doi.org/10.1063/1.5120816
Submitted: 21 July 2019 . Accepted: 30 September 2019 . Published Online: 08 October 2019

Norizzawati M. Ghazali, Hiroshi Tomizawa, Noriyuki Hagiwara, Katsuya Suzuki, Abdul M. Hashim, Tomohiro Yamaguchi, Seiji Akita, and Koji Ishibashi

Fabrication of tunnel barriers and single electron transistors in suspended multi-wall carbon nanotubes

Cite as: AIP Advances 9, 105015 (2019); doi: 10.1063/1.5120816
Submitted: 21 July 2019 • Accepted: 30 September 2019 •
Published Online: 8 October 2019

Norizzawati M. Ghazali,[1,2] Hiroshi Tomizawa,[1] Noriyuki Hagiwara,[1,3] Katsuya Suzuki,[1,3] Abdul M. Hashim,[1,2] Tomohiro Yamaguchi,[1,a)] Seiji Akita,[4] and Koji Ishibashi[1,5]

AFFILIATIONS

[1]Advanced Device Laboratory, RIKEN, 2-1 Hirosawa, Wako, Saitama 351-0198, Japan
[2]Malaysia-Japan International Institute of Technology, Universiti Teknologi Malaysia, Jalan Sultan Yahya Petra, Kuala Lumpur 54100, Malaysia
[3]Graduate School of Advanced Integration Science, Chiba University, Chiba 263-8522, Japan
[4]Department of Physics and Electronics, Osaka Prefecture University, 1-1 Gakuen-cho, Nakaku, Sakai, Osaka 599-8531, Japan
[5]RIKEN Center for Emergent Matter Science (CEMS), 2-1 Hirosawa, Wako, Saitama 351-0198, Japan

[a)]**Electronic mail:** tyamag@riken.jp

ABSTRACT

Fabrication processes have been developed to form the tunnel barriers in the suspended multi-wall carbon nanotubes (MWCNTs). Individual MWCNTs are positioned under the optical microscope to bridge them between the two metal electrodes. The tunnel barrier is formed by irradiating them with focused Ga ion beam (FIB), and its characteristics are evaluated with the resistance increase by the irradiation and the barrier height. It is found that those values depend not only on the dose of the Ga ions, but also on a diameter of the MWCNT. The single electron transistors (SETs) are fabricated by forming the double barriers in the suspended MWCNT. We find some devices show regular and stable SET behaviours.

I. INTRODUCTION

Carbon nanotubes are an attractive building block of the nanodevices because of their extremely small diameter that are realized in a self-assemble manner.[1] In addition to their electrical and optical applications,[2–4] their unique mechanical properties such as light mass and large stiffness are attractive for a high frequency resonator with a possible ultrasensitive mass sensing capability.[5–8] The nanotube mechanical resonator can be coupled with the single electron transistor (SET) for possible new functionalities.[9,10] The single-wall carbon nanotubes (SWCNTs) may be more advantageous than the multi-wall carbon nanotubes (MWCNTs) in terms of their much smaller diameter (~1 nm) compared to that ($\gtrsim$ 10 nm) for the MWCNT.[11] Besides, the SET can be simply fabricated in the SWCNT just by depositing the source and drain contacts, where the entire nanotube between the contacts could form the single quantum dot.[12,13] However, a big challenge for the SWCNT is to overcome a low reproducibility and reliability of the fabrication processes and to develop a technology to realize more complex and functional structures with multi-barriers.[14]

Despite their larger diameter, the MWCNT has the following advantages. First, it is easier to handle. Second, the resist process does not cause serious degradation of the material, while it often degrades the transport properties a lot in the case for the SWCNT.[15] To get around the problem, its growth has to be done in the final process so that the SWCNT is free from the resist contamination.[16,17] Third, the contact between the metal and the MWCNT is Ohmic even in the liquid He temperature,[18] which is in strong contrast to the SWCNT case where the Schottky barrier is usually formed and causes serious effects on the electron transport at low

temperatures. The Ohmic nature of the contact makes it possible to fabricate more functional multi-dot devices once the reliable and flexible tunnel barrier fabrication process is developed.[19] The use of ion beam irradiation in a wide range of energies has proven to be useful to functionalize the carbon nanotubes.[20] We reported the use of Ar ion beam irradiation through an opening of the electron beam resist to form the tunnel barriers,[21,22] and have recently shown that the focused ion beam (FIB) irradiation process is more reproducible and flexible.[23] In both cases, the MWCNTs were dispersed on a substrate from solution. In this paper, we demonstrate tunnel barrier formation in the suspended MWCNT with FIB and characterized the tunnel barrier in more detail when the diameter and the dose level were changed. Finally, the suspended SET in the MWCNT was demonstrated.

II. SAMPLE FABRICATION AND EXPERIMENTAL PROCEDURE

The MWCNTs used in this study were grown by an electric arc discharge method.[11,24] First, the source and drain electrodes were fabricated on the SiO_2/Si substrate by depositing palladium (Pd) metal with a thickness of 100 nm. The gap between the contacts was 500 nm. To fabricate the SET, the Pd gate electrode with a thinner thickness (~20 nm) was deposited in a separate process into the gap between the source and drain electrodes. The positioning process to locate individual MWCNTs is schematically shown in Fig. 1(a)–(f). The method is similar to the one we used to locate individual semiconductor nanowires.[25] The polyvinyl alcohol (PVA) was spin coated on a separate Si substrate, followed by the spin-coating of polymethyl methacrylate (PMMA) (Fig. 1(a)), and the MWCNTs were dispersed on it (Fig. 1(b)). Then, the PMMA film with the MWCNTs was peeled off the Si substrate using the thermal tape (Fig. 1(c)), and transferred onto the SiO_2/Si substrate with the metal electrodes. In this transfer process, the position of the MWCNT could be precisely monitored under the optical microscope to bridge it between the electrodes (Fig. 1(d)). After that, the thermal tape was removed and the PMMA film was dissolved in acetone at room temperature (RT). The two-terminal resistance was measured at RT before the FIB irradiation, and the MWCNT was observed using a scanning electron microscope (SEM) to check the gap between the electrodes was clean. Diameters of MWCNTs were also evaluated by the SEM within an error of ±2 nm. A minimum diameter of the MWCNT that could be manipulated in the present process was about 20nm because the positioning was carried out using the optical microscope. The most of the MWCNTs manipulated in the present study had a diameter roughly ranging from 30 nm to 50 nm. In the case of the dispersed MWCNTs on the substrate, their diameters were 10 ~ 20 nm because SEM could be used to find their position.

A tunnel barrier was formed in the MWCNT by a single scan of Ga FIB with an acceleration voltage of 40 kV as illustrated in

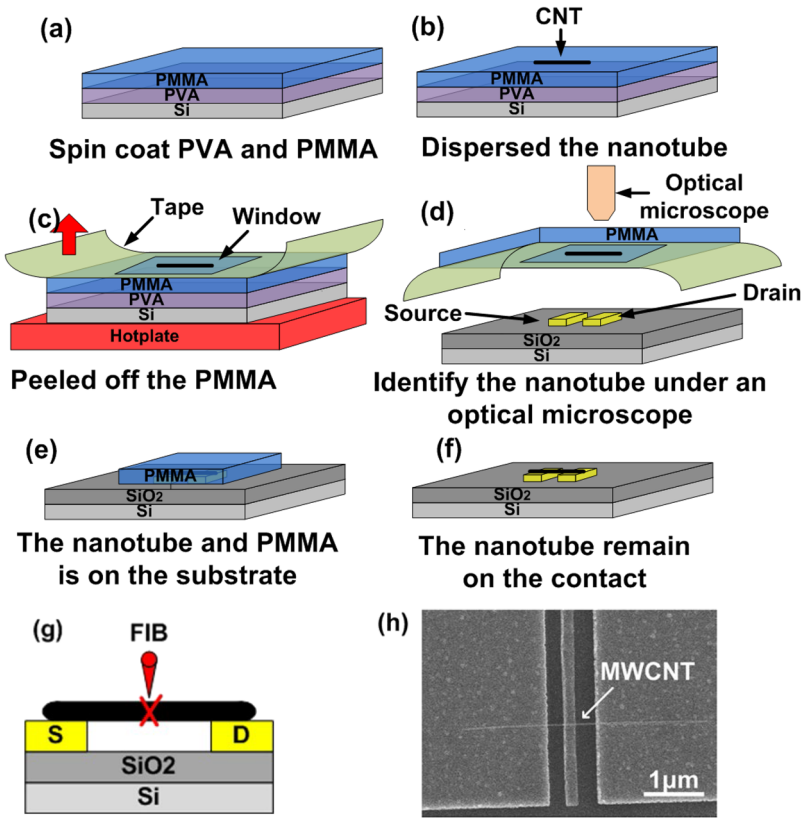

FIG. 1. (a)-(f) Schematic images of fabrication process flow of the suspended MWCNTs. (g) Schematic image of FIB irradiation on a suspended MWCNT. (h) SEM image of the fabricated device with a gate.

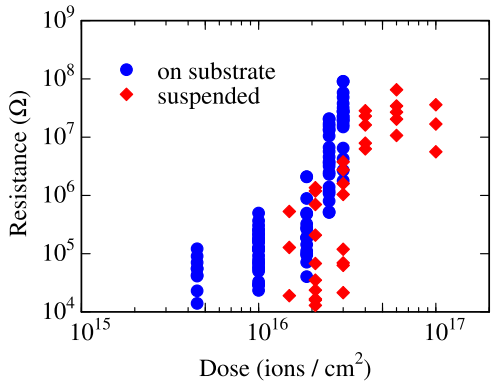

FIG. 2. RT resistance after the FIB irradiation with various doses. Data for the suspended samples (solid red diamond) is shown together with the samples fabricated on a substrate (solid blue circle[23]) for comparison. Samples with various diameters were irradiated with a same dose level.

Fig. 1(g). Figure 1(h) shows a SEM image of the fabricated suspended MWCNT. The two-terminal resistance measurements before and after the ion irradiation were carried out at RT using micro probers connected to a source-measure unit. The current-voltage (I-V) characteristics of the two-terminal suspended MWCNT were measured in various temperatures between 1.5 K and RT to determine the barrier height.[22] Coulomb diamond measurements (current as functions of a source-drain voltage and a gate voltage) and Coulomb oscillation measurements (Current as a function of the gate voltage for the small and fixed source-drain voltage) were carried out for the double barrier samples at around 1.5 K.

III. RESULTS AND DISCUSSION

A. Characteristics of the single barrier

The two-terminal resistance of most of the measured MWCNTs was found to be in a range of 10 kΩ to 20 kΩ at RT for all the suspended samples before the FIB irradiation. From rough estimation using three and four terminal measurements, we found the contact resistance varied in a range of several kΩ from sample to sample. These resistance values were similar with those fabricated on the substrate, as we reported previously.[22] In our previous report,[23] we found that the overall effect of the FIB irradiation was the resistance increase as the dose was increased (Data are replotted by the blue solid circles in Fig. 2). The similar experiments were carried out for the suspended MWCNTs, and the data are shown in the red solid rectangles in Fig. 2.

Again in this case, the resistance increased by a few orders of magnitude as the dose was increased. We should note that in both cases, the MWCNTs with various diameters are included in the figure, and as we will show later in detail, the diameter variation is a dominant reason for the observed large resistance variation in the samples irradiated with a same dose.

It can be noted that the overall data points for the case of suspended samples are slightly shifted to the right, which means that the resistance increase is smaller for the suspended samples, compared with samples on the substrate, when they are irradiated with a similar dose. In the case of the MWCNTs on the substrate, the randomly backscattered Ga ions may cause an additional damage to the MWCNT, while the effect may be ignored for the suspended MWCNTs. This could be a possible reason. But, as will be shown in a later section, the diameter dependent damage can be another possible reason, meaning that the resistance increase is larger as the diameter is reduced. We should recall that the suspended MWCNTs had larger diameters, compared with the MWCNTs on the substrate.

To investigate the origin of the large variation of the resistance increase for the same doses, observed in Fig. 2, its diameter dependence was measured. Figure 3 shows the diameter dependence of the resistance after the irradiation for (a) high and (b) low dose levels, where the high and low doses correspond to 6.0×10^{16} ions/cm^2 and 2.1×10^{16} ions/cm^2, respectively. It is found that the resistance increase strongly depends on the diameter, as was reported previously in Refs. 26 and 27. In both high and low dose cases, the resistance increase is larger as the diameter is reduced.

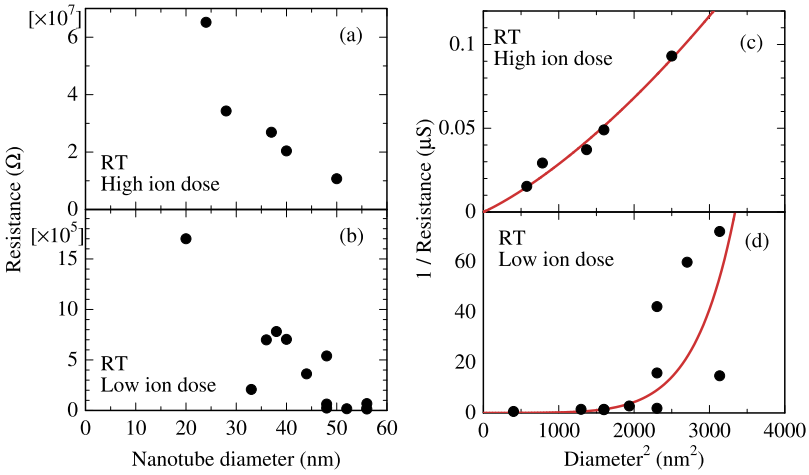

FIG. 3. RT resistance after the FIB irradiation as a function of the diameter for fixed dose levels of (a) 6.0×10^{16} ions/cm^2 (High dose) and (b) 2.1×10^{16} ions/cm^2 (Low dose). Same data are re-plotted in (c) and (d) for the high and low dose cases to show the conductance (1/resistance) as a function of a square of the diameter. The solid curves are calculated one based on the expression shown in the text (Eq. (1)). For the high dose case, $a = -0.013$ nm^{-1}, $b = 4.2$, and for the low dose case, $a = -0.18$ nm^{-1} and $b = 8.9$, where $\phi_b(d)/k_BT = ad + b$ (d is a diameter) was assumed.

To get more insight on the diameter dependence, in Fig. 3(c) and (d), we plot, using the same data, the conductance (1/resistance) as a function of the squared diameter (d^2), in order to see if the simple geometrical effect holds based on the Ohm's law, $G = I/V = \sigma A/L \sim d^2$, where σ is a conductivity, L the length, and $A \sim d^2$ the cross-sectional area of the irradiated region. We can ignore the series resistances of the MWCNT-metal contacts and non-irradiated regions except some samples with resistance less than 10 kΩ, so that we can reasonably assume the measured resistance represents that of the irradiated region except those with the low resistance. It is reported in Ref. 27 that the FIB irradiation can cause even drastic cutting or thinning of the MWCNT, depending on the diameter and the dose level. However, looking into the dose levels and diameters used in our experiments, we conclude these drastic changes are not happening in our samples. The effect of the FIB irradiation in our conditions is to make the irradiated region amorphous, as we showed in the previous report,[23] so that the diameter remains same after the FIB irradiation. For the high dose case in Fig. 3(c), the conductance is nearly proportional to d^2, indicating that the irradiated region almost follows the Ohm's law. This means that σ of the irradiated region is almost independent of d. But, for the low dose case in Fig. 3(d), it does not. We will come back to this point later and will show that the behaviours can be understood by a simple tunnel barrier model that includes an observed diameter dependence of the tunnel barrier height.

To estimate the tunnel barrier height and to see how it depends on a diameter and the dose, the current was measured in various temperatures for the small source-drain voltage, and was plotted as a function of $1/T$ (Arrhenius plot). A typical plot is shown in Fig. 4(a), where the current increases exponentially in this temperature region. This behaviour is understood by the simple single rectangular tunnel barrier model. The thermally excited over-the-barrier current is dominant in the indicated temperature range.[23,28] From the slope, the barrier height, ϕ_b, can be obtained. In Fig. 4(b) and (c), ϕ_b and resistance after the FIB irradiation are plotted as a function of (b) dose with a fixed diameter (~ 40 nm) and (c) a diameter with a fixed dose (2.1×10^{16} ions/cm^2). As expected, ϕ_b increases as the dose is increased when the diameter is fixed (Fig. 4(b)). As seen in Fig. 4(c), it also strongly depends on the diameter even in its small range (~ 15 nm) when the MWCNTs are irradiated with the same dose. The absolute diameter range appears to be small, but the variation range is ~30% of the diameters, which may not be small. This is again an origin of the resistance variation of the samples irradiated with a same dose (Fig. 2). Although we do not have enough data to discuss about microscopic details or the nature of the damage in the irradiated region, the observations suggest that the effect of the FIB irradiation or damage depends on the diameter as well as the dose, meaning ϕ_b depends on the diameter and a dose in the simple single barrier model. As seen in Fig. 5, the plot of the resistance vs ϕ_b for both the suspended samples and the samples on the substrate appears to indicate that the resistance is dominantly scaled by ϕ_b.

Now, we come back to Fig. 3(c) and (d) to explain the diameter dependence of the conductance for high and low dose levels. The conductance, $G = 1/R$, at a small source drain voltage could be simply described by a following expression,

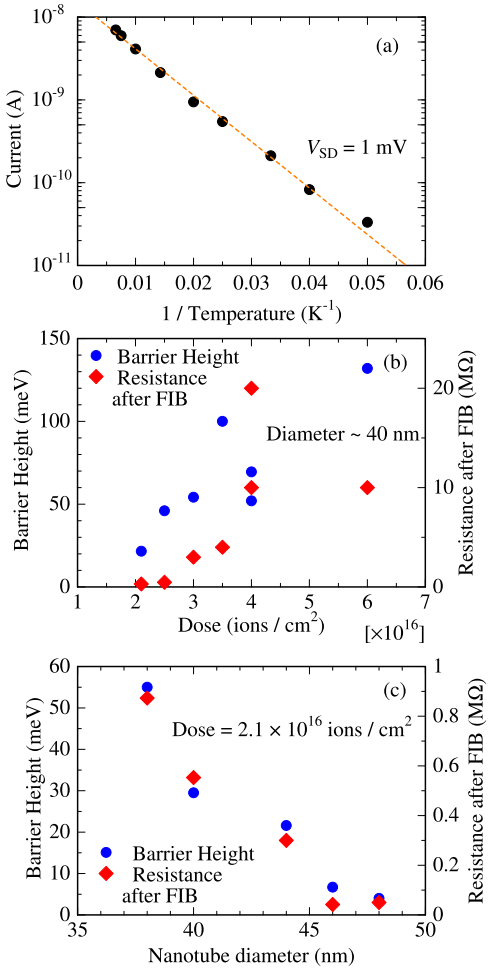

FIG. 4. (a) Current with a small source-drain voltage (V_{sd} = 1 mV) as a function of inverse temperature (Arrhenius plot) for a typical sample (diameter ~ 33 nm, dose = 2.1×10^{16} ions/cm^2) (b) Resistance after the FIB irradiation and the barrier height as a function of the dose. (c) Resistance after the FIB irradiation and the barrier height as a function of a diameter.

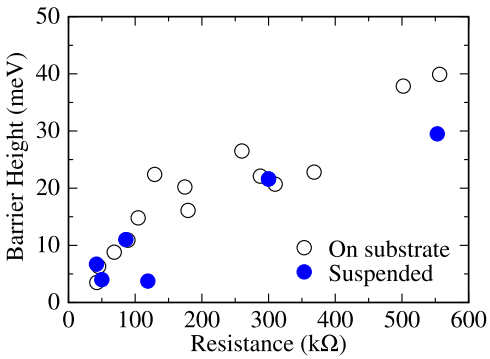

FIG. 5. Barrier height as a function of the resistance after the FIB irradiation. Data for the suspended samples (Solid blue circle) are shown together with the samples on a substrate (open circle[23]) for comparison.

$$G \sim \sigma d^2/L \propto d^2\left(C_{th}\, exp\left(-\frac{\phi_b}{k_B T}\right) + C_{tu}\right) \quad (1)$$

where d is a diameter of the MWCNT, ϕ_b the barrier height and k_B the Boltzmann constant. The first term represents a contribution of the over-the-barrier current due to the thermally excited carriers with a constant, C_{th}, and the second term represents a contribution by the tunneling process with a constant, C_{tu}. It should be noted that the barrier height, ϕ_b, depends on the diameter, d, in the present experiment. At RT, the thermal contribution of the first term is dominant for all samples we measured, so that we ignore the second term at RT for the fitting.

The solid curves in Fig. 3(c) and (d) are the fits based on the above model expression. For the low dose case, $\phi_b(d)$ is phenomenologically assumed to be a simplest form as $\phi_b(d)/k_BT = ad + b$ with data shown in Fig. 4(c), where $a = -0.18\ nm^{-1}$ and $b = 8.9$. For the high dose case, the diameter dependence of the barrier height, which corresponds to Fig. 4(c), was not available except one data point in Fig. 4(b) (6.0×10^{16} ions/cm^2) because, for most of the samples irradiated with this dose level, the resistance was too high at the low temperatures to measure the temperature dependence and get the barrier height. The only one data point was used to obtain the fitting curve in Fig. 3(c) with $a = -0.013\ nm^{-1}$ and $b = 4.2$. In both cases, the model calculations qualitatively explain the experimental data very well. The large conductance variation observed in $d^2 > 20 \times 10^{-16}$ m^2 for the low dose case (Fig. 3(d)) arises from the small barrier height, the fluctuation of which causes large conductance variation. It is interesting to note that "a" is much smaller for the high dose case, compared to the value for the low dose case. This means that the diameter dependence of the barrier height is much weaker in the high dose case, while it strongly depends on the diameter for the low dose case as seen in Fig. 4(c). A simple thought may lead to the diameter independent barrier height as is the case for the high dose level, but the diameter dependent barrier height observed in the low dose level needs further microscopic study of the irradiated region.

B. Characterization of the single electron transistor (SET)

The single electron transistors were fabricated in the individual MWCNTs by forming two tunnel barriers by the FIB irradiation. The separation between the irradiated regions was set to be 100 nm, and the Pd metal gate was pre-deposited underneath the MWCNT. Figure 6(a) and (b) are regular Coulomb diamonds and Coulomb oscillations at 1.5K for some particular sample, and from these, the charging energy, E_c and gate capacitance, C_g are estimated to be around ~ 6 meV and ~ 1.6 aF, respectively.[29,30] The Coulomb oscillations were successfully observed up to ~ 10 K (0.9 meV), which is consistent with a required condition, $k_BT \ll E_c$. Clear SET feature is also observed for other several samples, so we believe that our FIB technique is applicable to fabricate SETs of suspended MWCNTs as well as the ones on a substrate.[23] It should be noted about the reproducibility of the Coulomb oscillations. In Fig. 6(b), Coulomb oscillations obtained in two separate gate scans with same conditions are plotted. As seen in the figure, positions of the two oscillations are reproducible, but the height of the current peaks is different in the two measurements. This has been observed in some other samples, and it is because the peak current should be more sensitive than the period to environmental conditions such as impurities and traps that may exist in or near the MWCNT.

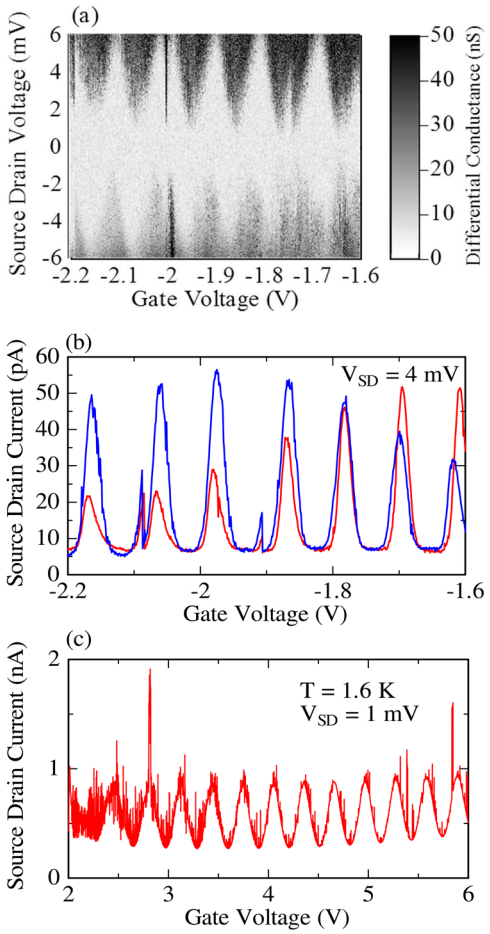

FIG. 6. (a) Grey scale plot of the differential conductance as functions of source-drain voltage (V_{sd}) and the gate voltage (V_g) (Coulomb diamonds). (b) Current as a function of the gate voltage (V_g) (Coulomb oscillations) for two identical gate sweeps (V_{sd} = 4mV). Measurements are done at 1.5 K. (c) Coulomb oscillations with spike-like noise in another sample. Measurements are done at 1.6 K.

In some samples, spike-like noise was observed on the drain current on top of the regular and reproducible Coulomb oscillations, as shown in Fig. 6(c). This noise was not observed in the samples fabricated on a substrate. Moreover, it was not observed for the suspended MWCNTs with a single barrier. Therefore, it seems that the spike-like noise may appear only in the suspended MWCNT with double-barriers. Considering that the SET is a very sensitive charge sensor, it may be caused by a combination of mechanical instability and time-dependent charge traps near the dot region. Further study and improvement of fabrication process is necessary to remove the noise.

IV. CONCLUSION

The individual and suspended MWCNTs have been fabricated with a mechanical transfer technique, and the tunnel barriers were

formed on them by the local FIB irradiation. It was found that the resistance of the irradiated region depended on the dose of the FIB irradiation and a diameter of the MWCNT. The tunnel barrier height was estimated by the temperature dependence of the current with a small source drain voltage, and was found to scale roughly with the resistance. The single electron transistors were fabricated in the suspended MWCNT by forming the two tunnel barriers. The regular Coulomb diamonds and Coulomb oscillations, typical behaviours to the single dot, were observed in some samples, but the spike-like noise was observed in other samples, superimposed on the regular Coulomb oscillations. The noise appears to be unique to the suspended SET, which has to be eliminated for the device applications of the structure.

ACKNOWLEDGMENTS

The authors would like to thank for the supports provided by CEMS Materials Characterization Support Unit in RIKEN. N. M. Ghazali thanks the International Program Associate (IPA) and Malaysia-Japan International Institute of Technology (MJIIT) for the scholarship. This work was partially supported by a MEXT Grant-in-Aid for Scientific Research on Innovative Areas 'Science of Hybrid Quantum Systems'.

REFERENCES

[1] K. Ishibashi, S. Moriyama, D. Tsuya, T. Fuse, and M. Suzuki, J. Vac. Sci. Technol. **24**, 1349 (2006).
[2] A. D. Franklin, M. Luisier, S.-J. Han, G. Tulevski, C. M. Breslin, L. Gignac, M. S. Lundstrom, and W. Haensch, Nano Lett. **12**, 758 (2012).
[3] P. Avouris, M. Freitag, and V. Perebeinos, Nat. Photonics **2**, 341 (2008).
[4] A. Högele, C. Galland, M. Winger, and A. Imamoğlu, Phys. Rev. Lett. **100**, 217401 (2008).
[5] V. Sazanova, Y. Yaish, H. Ustunel, D. Roundy, T. A. Arias, and P. L. McEuen, Nature **431**, 284 (2004).
[6] D. Garcia-Sanchez, A. San Paulo, M. J. Esplandiu, F. Perez-Murano, L. Forró, A. Aguasca, and A. Bachtold, Phys. Rev. Lett. **99**, 085501 (2007).
[7] K. Jensen, K. Kim, and A. Zettl, Nat. Nanotechnol. **3**, 533 (2008).
[8] H. Y. Chui, P. Hung, H. W. Ch. Postma, and M. Bockrath, Nano Lett. **8**, 4342 (2008).
[9] B. Lassagne, Y. Tarakanov, J. Kinaret, D. Garcia-Sanchez, and A. Bachtold, Science **325**, 1107 (2009).
[10] P. Häkkinen, A. Isacsson, A. Savin, J. Sulkko, and P. Hakonen, Nano Lett. **15**, 1667 (2015).
[11] S. Iijima, Nature **354**, 56 (1991).
[12] M. Bockrath, D. H. Cobden, P. L. McEuen, N. G. Chopra, A. Zettl, A. Thess, and R. E. Smalley, Science **275**, 1922 (1997).
[13] K. Ishibashi, M. Suzuki, T. Ida, K. Tsukagoshi, and Y. Aoyagi, Jpn. J. Appl. Phys. **39**, 7053 (2000).
[14] A. Hida and K. Ishibashi, Appl. Phys. Express **8**, 045101 (2015).
[15] S. M. Khamis, R. A. Jones, and A. T. Charlie Johnson, AIP Advances **1**, 022106 (2011).
[16] J. Cao, Q. Wang, and H. Dai, Nat. Mater. **4**, 745 (2005).
[17] G. A. Steele, G. Gotz, and L. P. Kouwenhoven, Nat. Nanotechnol. **4**, 363 (2009).
[18] C. Schönenberger, A. Bachtold, C. Strunk, J.-P. Salveta, and L. Forró, Appl. Phys. A **69**, 283 (1999).
[19] K. Ishibashi, D. Tsuya, M. Suzuki, and Y. Aoyagi, Appl. Phys. Lett. **82**, 3307 (2003).
[20] J. A. V. Pomoell, A. V. Krasheninnikov, K. Nordlund, and J. Keinonen, J. Appl. Phys. **96**, 2864 (2004).
[21] M. Suzuki, K. Ishibashi, T. Toratani, D. Tsuya, and Y. Aoyagi, Appl. Phys. Lett. **81**, 2273 (2002).
[22] H. Tomizawa, T. Yamaguchi, S. Akita, and K. Ishibashi, J. Appl. Phys. **118**, 044306 (2015).
[23] H. Tomizawa, K. Suzuki, T. Yamaguchi, S. Akita, and K. Ishibashi, Nanotechnology **28**, 165302 (2017).
[24] T. W. Ebbesen and P. M. Ajayan, Nature **358**, 220 (1992).
[25] R. Wang, R. S. Deacon, D. Car, E. P. A. M. Bakkers, and K. Ishibashi, Appl. Phys. Lett. **108**, 203502 (2016).
[26] B. Q. Wei, J. D'Arcy-Gall, P. M. Ajayan, and G. Ramanath, Appl. Phys. Lett. **83**, 3581 (2003).
[27] M. S. Raghuveer, P. G. Ganesan, J. D'Arcy-Gall, and G. Ramanath, Appl. Phys. Lett. **84**, 4484 (2004).
[28] R. Martel, V. Derycke, C. Lavoie, J. Appenzeller, K. K. Chan, J. Tersoff, and P. Avouris, Phys. Rev. Lett. **87**, 256805 (2001).
[29] L. P. Kouwenhoven, C. M. Marcus, P. L. McEuen, S. Tarucha, R. M. Westervelt, and N. S. Wingreen, *Mesoscopic electron transport* (Springer, Netherlands, 1997).
[30] D. V. Averin and K. K. Likharev, in *Microscopic Phenomena in Solids*, edited by B. Altshuler *et al.* (Elsevier, Amsterdam, 1991).